Int. J. Heat Mass Transfer. Vol. 34, No. 9, pp. 2395–2408, 1991
Printed in Great Britain

0017–9310/91 $3.00+0.00

The influence of the freezing process on vapour transport during sublimation in vacuum-freeze-drying

M. KOCHS, CH. KÖRBER, B. NUNNER and I. HESCHEL
Helmholtz-Institut für Biomedizinische Technik an der RWTH Aachen,
Pauwelsstraße 30, D-5100 Aachen, Germany

(*Received* 23 *March* 1990)

Abstract—The influence of the freezing process on mass transfer during subsequent sublimation in an aqueous polymer solution is investigated. Different textures of the frozen sample depending on the solidification parameters and the texture dependent diffusion coefficient for vapour transport out of the frozen, drying sample are studied. Experiments are performed, using a controlled directional solidification method (Bridgman technique) and isothermal sublimation, analysed through a light microscope. The dependence of the 'ice finger' primary spacing λ_1 with the solidification parameters $v_{il}^{-1/4} \cdot G^{-1/2}$ (solidification interface velocity and temperature gradient, cf. Hunt, *Solidification and Casting of Metals, Proc. Int. Conf. on Solidification*, Sheffield, U.K., pp. 3–9. The Metals Society (1979); Kurz and Fisher, *Acta Metall.* **29**, 11–20 (1981)) is shown. A proportionality between this combination of freezing parameters and the diffusion coefficient for vapour transport during sublimation is confirmed by the experiments.

INTRODUCTION

FREEZE-drying is a preservation method for products which quickly deteriorate in the presence of humidity at ambient temperature. The sample which usually contains an aqueous solution is initially frozen under ambient pressure in the first step of the preservation process. As most solutes are generally not included in the ice crystal, the solvent water is transformed to pure ice and the solutes are concentrated in the residual liquid. After solidification, there exist regions of pure ice and of concentrated solutes in the sample, the concentrated solutes being in a eutectic or vitrified state. The geometric distribution of these regions in the sample, the solidification pattern or texture, strongly depends on the way freezing is performed. After the solidification step a vacuum is applied to the sample. Primary drying, mainly the transformation of ice into vapour by sublimation, and after that secondary drying, the desorption of water bound to the ice-free sample, takes place. As long as no collapse (cf. ref. [1]) of the already ice-free part of the sample occurs, the space previously occupied by the ice crystals becomes the main passageway for vapour transport out of the specimen into the environment (e.g. ref. [2]). Different morphologies of the solidification texture may result depending on the chosen solidification parameters. These different textures then lead to different resistances against the vapour transport during drying. The freezing process thus has a strong influence on the entire freeze-drying procedure.

The quality of the final freeze-dried product is greatly influenced by the freezing process. For instance, the freezing process controls the colour and the flavour of freeze-dried coffee extract [3] or the retention of volatile compounds [4]. Proteins or cells, subjected to freeze-drying, can be damaged during the freezing process already [5]. So on the one side the susceptibility of the product to cooling and freezing imposes certain requirements on the method by which the sample has to be frozen at the beginning of freeze-drying.

On the other hand if the product allows a certain variation of the freezing parameters the freezing process can be designed for obtaining a desired behaviour of the sample during the primary and secondary drying process stages or to influence its texture in order to get a favourable rehydration behaviour. Several publications report about the mass transfer during freeze-drying and about experimental [6–9] as well as theoretical [2, 10–13] investigations on this subject. The influence of the freezing procedure on mass transfer during the subsequent sublimation process was also examined by some authors experimentally [7, 9, 14]. These experiments were performed in bulk samples. The solidification process was characterized by describing the technical way the sample was cooled or by stating a cooling rate, i.e. temperature decrease per unit time, measured somewhere inside the sample. As the solidification conditions in bulk samples usually vary with the location inside the sample [15, 16] due to a variation of interface velocity or temperature gradient at the interface, these samples generally exhibit a non-uniform solidification texture. Under these circumstances it was thus possible to determine overall mass transfer coefficients from drying rates for different freezing conditions.

In this work an attempt is made to correlate the mass transfer behaviour in a freeze-drying sample

NOMENCLATURE

B	cooling rate [K m^{-1}]
D	diffusion coefficient for vapour transport through the void fraction of the sample [m^2 s^{-1}]
D_K	diffusion coefficient of gas at high Knudsen numbers [m^2 s^{-1}]
D_l	diffusion coefficient in the liquid [m^2 s^{-1}]
G	mean temperature gradient at the ice–liquid interface in the direction of ice finger growth [K m^{-1}]
G_l	temperature gradient on the liquid side of the ice–liquid interface [K m^{-1}]
G_s	temperature gradient on the solid side of the ice–liquid interface [K m^{-1}]
G^*	temperature gradient imposed on the sample in directional solidification experiments [K m^{-1}]
k	distribution coefficient [—]
Kn	Knudsen number [—]
L	mean free path length [m]
M	molecular weight [kg kmol^{-1}]
M_{H_2O}	molecular weight of water [kg kmol^{-1}]
n	number of molecules per unit volume [m^{-3}]
N_v	mass flux of vapour through the void fraction of the sample [kg m^{-2} s^{-1}]
p_{iv}	vapour pressure at the interface [Pa]
p_v	vapour pressure [Pa]
r_e	effective radius [m]
R_m	universal gas constant [J kmol^{-1} K^{-1}]
R_v	gas constant of vapour [J kg^{-1} K^{-1}]
t	time [s]
T	absolute temperature [K]
T_c	collapse temperature [°C]
ΔT_0	temperature difference between equilibrium freezing temperature and temperature of complete solidification [K]
v	velocity of solidification interface (general case) [m s^{-1}]
v_{il}	velocity of the ice–liquid interface [m s^{-1}]
v^*	pushing velocity in directional solidification experiments [m s^{-1}]
x	coordinate; origin at the sample surface and measured in the direction of sublimation interface movement [m]
x_{iv}	position of the ice–vapour interface [m].

Greek symbols

Γ	Gibbs–Thomson coefficient [K · m]
δ	diameter of vapour molecules [m]
κ_l	thermal conductivity in the liquid phase [W m^{-1} K^{-1}]
κ_s	thermal conductivity in the solid phase [W m^{-1} K^{-1}]
λ_1	primary spacing, i.e. mean distance between neighbouring dendrites or cells [m]
ρ_i	density of ice [kg m^{-3}]
ρ_v	density of water vapour [kg m^{-3}]
ϕ	angle between the growth direction of ice fingers and the geometric axis of the sample capillary [—].

more directly to the freezing conditions. This includes the consideration of the morphology of the ice–liquid interface during solidification, the texture resulting after complete freezing, and the influence of this texture on the mass-transfer properties during drying. For this purpose, experiments are performed to produce a well controlled and reproducible uniform solidification morphology with the aid of the so-called Bridgman technique of solidification, and with light microscopic observation of the dynamics of the solidification process. After complete freezing, the frozen samples with the uniform and regular texture are dried by sublimation under isothermal conditions and also subjected to light microscopic observation. The evaluation of these experiments yields a description of the correlation between the appropriate freezing parameters, i.e. temperature gradient and velocity of the solidification interface, and the resulting mass transfer coefficients during the sublimation process. The superposition of the thus determined relationship between freezing parameters and sublimation mass transfer properties on the instationary freezing conditions found in bulk freeze-drying should give a much more accurate possibility to predict the drying behaviour in a bulk sample, with a given freezing process, or to design a freezing process to improve or optimize the drying behaviour and the rehydration properties.

THEORETICAL CONSIDERATIONS

Inner texture of a frozen sample

When considering the influence of the solidification process on mass transfer during sublimation, the most relevant aspect of the solidification process is the texture obtained upon its completion. During solidification an ice–liquid interface advances through the sample. The inner texture of the sample after complete solidification first of all is closely related to the morphology of the ice–liquid interface in the course of freezing.

Theoretically, solidification may result in different patterns: the interface may be planar, i.e. smooth and flat, cellular (columnar) or dendritic, i.e. needle, tongue or finger-shaped, or tree-like with side

branches. As first described by Rutter and Chalmers [17] for alloys, a necessary (but not sufficient) criterion for the instability of the planar interface and the subsequent breakdown to a more complex structure is the so-called constitutional supercooling (cf. also ref. [18]). The solute concentration gradient building up ahead of the advancing interfaces has a destabilizing effect whereas the thermal gradient stabilizes. In the special case of aqueous solutions, the situation is largely characterized by the nearly vanishing distribution coefficient for most solutes [19], their almost complete exclusion from the growing ice lattice, resulting in a steadily increasing and destabilizing concentration gradient [20–22]. A planar ice front is hence only achieved in special cases for a limited period of time, i.e. in the presence of a very high temperature gradient and/or at low ice front velocities [21–23]. The conditions for the planar form of solidification are hardly ever found in the bulk freezing of aqueous solutions [24].

A large portion of most freezing processes used in freeze-drying may be regarded as directional solidification, i.e. the growth direction of the solidification interface is opposite to the main heat flow direction. In the case of cellular solidification most of the ice fingers are arranged parallel to each other and the growth direction and a characteristic trunk spacing λ_1, i.e. the distance between the geometric axes of two neighbouring ice fingers, may be defined (cf. Fig. 1).

Depending on the growth conditions, the ice fingers formed at the non-planar interface are termed cells or dendrites. According to Kurz and Fisher [18] the so-called cells are crystals, characterized by the axes of the trunks to be preferably parallel to the direction of the heat flux. Dendrites are crystalline forms which adopt an orientation which is as close as possible to the main heat flux direction, but follows one of the preferred crystallographic growth axes. Behind a short tip region, secondary perturbations may develop on the shoulder of the initially smooth dendrite. These perturbations may grow and form side branches. Especially in the case of dendritic growth with the formation of side branches, the structure may be altered by coarsening after the initial solidification step.

An equation for the primary spacing λ_1 developing in a binary solution during directional solidification may be derived with the following main assumptions (cf. Fig. 1): the dendrite shape to be an ellipsoid of revolution in a plane parallel to the growth direction, the arrangement of the neighbouring dendrites to be hexagonal in a plane perpendicular to the growth direction [25]

$$\lambda_1 = 4.3\left(\frac{D_1 \Gamma \Delta T_0}{k}\right)^{1/4} v^{-1/4} G^{-1/2} \qquad (1)$$

where D_1 is the diffusion coefficient of the solute in the liquid [$m^2 s^{-1}$], Γ the Gibbs–Thomson coefficient [K · m], k the distribution coefficient, ΔT_0 the difference between equilibrium freezing temperature and temperature of complete solidification [K], v the velocity of the ice–liquid interface [$m s^{-1}$] and G the temperature gradient at the ice–liquid interface [$K m^{-1}$].

For many cases of application some of the material properties used in the above equation (like the Gibbs–Thomson coefficient Γ) will not be available. For this reason, only the functional dependence on the solidification parameters, v and G, in the above equation will be used here

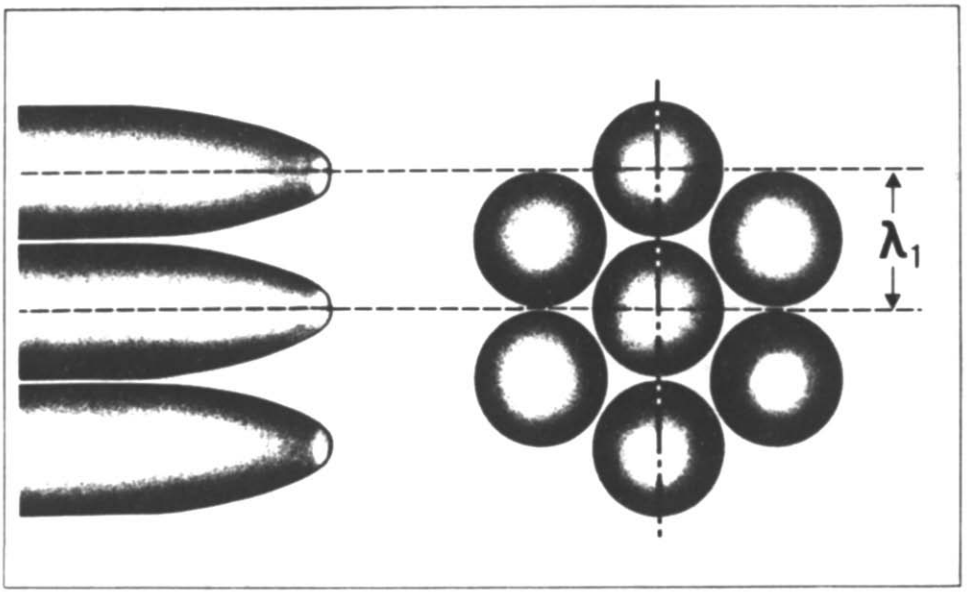

FIG. 1. Sketch of the geometric arrangement of the ice fingers at the ice–liquid interface, as seen normal (left) and parallel (right) to the growth direction.

$$\lambda_1 \propto v^{-1/4} G^{-1/2}. \quad (2)$$

The growth velocity thus has a smaller effect upon λ_1 than does a change in the temperature gradient. It should be noted in particular that the solidification pattern is governed by these two parameters, and not, as frequently described, by the cooling rate, which is $B = -Gv$ in case of directional solidification (cf. ref. [18]). A complete description of the geometric form of dendrites or cells in freezing aqueous solutions is difficult to achieve because of the complexity of the theoretical models. Another complication results from the anisotropy of growth of the ice crystal. Our own experiments [26] and descriptions of the geometry of ice crystals growing into supercooled water [27] bear the assumption that the cross-section of the growing dendrites, perpendicular to the growth direction, is elliptic. After the freeze-drying of an aqueous potato-starch solution Spieß [6] found the geometry of the void channels to be rectangular to hexagonal, depending on the initial concentration, the geometry of the channels of a freeze-dried white of egg aqueous solution to be cylindrical. These considerations led us to the assumption that the cross-section of the ice fingers as long as they grow without interaction with neighbouring fingers to be elliptic or circular. When the ice fingers subsequently grow closer to each other the cross-section might change to a more or less rectangular or hexagonal shape. Because of the lack of exact information on the geometry, and because we believe that it is sufficient for our present purposes, in the following we shall assume a circular shape of the cross-section of the growing ice fingers perpendicular to the growth direction and of the void channels left after sublimation. We also do not consider the case of a tree-like structure with side branches unless indicated.

Mass transfer during sublimation

During primary drying, vapour is transported from the sublimation interface through the already dried part of the sample to the vacuum chamber. When mass transfer through the dry part of the sample, where ice crystals were present after solidification, is considered, mass transfer may be regarded as mass transfer through fine pores (e.g. ref. [2]).

Depending on the properties of the gases present and on geometrical factors different mechanisms of mass transfer have to be considered in this problem. The dimensionless number specifying the regime of mass transfer is the Knudsen number Kn. It is the mean free path of the molecules L related to the pore diameter $2r_c$

$$Kn = \frac{L}{2r_c}. \quad (3)$$

For small Knudsen numbers, this means that the mean free path is short in comparison to the pore diameter, ordinary or bulk diffusion or viscous flow may be present, depending on the amount of an inert gas present in the pores. For large Knudsen numbers molecular diffusion, also called Knudsen diffusion, is present. For this kind of diffusion, when the molecules collide much more frequently with the walls of the pore than with each other, the kinetic theory of gases provides the following expression for the diffusion coefficient in a long cylindrical tube (e.g. ref. [28]):

$$D_K = \frac{2r_c}{3}\sqrt{\left(\frac{8R_m T}{\pi M}\right)} \quad (4)$$

where D_K is the diffusion coefficient of a gas at high Knudsen numbers [$m^2 s^{-1}$], R_m the universal gas constant [$J kmol^{-1} K^{-1}$], T the absolute temperature [K] and M the molecular weight [kg $kmol^{-1}$].

In addition to the mass transport in the pores, surface diffusion, i.e. the flow of molecules adsorbed by the surface of the walls of the pores, may be present. Any flow in excess of the theoretical Knudsen flow, may be attributed to surface diffusion (e.g. ref. [28]).

EXPERIMENTAL PROCEDURE

As mentioned above, bulk freezing in almost all cases produces a solidification morphology varying with the location in the sample. In this work we have chosen a solidification method that insures that the solidification morphology is not changing with the location in the sample and therefore rendering the possibility to look at the sublimation process in a uniform and regular matrix of ice and concentrated solutes.

The solution used in the experiments consists of 10 wt% hydroxyethyl starch (HES) in water (specification of the dry HES powder (supplied by Leopold GmbH Austria): degree of substitution D.S. = 0.62, molecular weight (weight average value) $M_w = 200\,000$ g mol^{-1}, NaCl content = 0.19 wt% (measured by flame photometry), water content $\approx$ 3.8 wt% (measured by evaporation to dryness followed by weighing (cf. ref. [29])))). The polymer HES is chosen as a model solution for the experiments because some work was performed in our group on the freezing behaviour of aqueous solutions containing this substance [30, 31], on the synthesis and analysis of HES [29] and on the alteration of the local distribution of HES in a solution by a directional freezing process in bulk samples (unpublished work). This renders the possibility of using existing data and methods when performing the described experiments and will help to apply the obtained results to bulk samples. Like other macromolecular freeze-drying additives (e.g. Dextran, Ficoll or polyvinylpyrrolidone (cf. ref. [1])), aqueous solutions of HES show a relatively high collapse temperature (i.e. the breakdown of the dry product structure at the ice-vapour interface when a certain temperature is exceeded) of $T_c \approx -15°C$ (own measurements). This allows for a high freeze-drying temperature.

A method generating a stationary solidification

process is the so-called Bridgman type of solidification, where the sample is moved with a constant velocity v^* through a temperature field with a constant temperature gradient G^* and both parameters can be adjusted and varied independently.

Sublimation in the described experiments is performed under isothermal conditions with respect to time and space. This implies that the temperature and, assuming equilibrium conditions, the vapour pressure at the sublimation interface are fixed. The temperature of the diffusion pathway is also fixed, allowing a simple and accurate evaluation of the experiments.

In contrast to experiments in bulk samples, where the container and the sample itself (when exceeding a certain thickness) are normally opaque, freezing and drying, in the experiments described below, are performed in thin glass capillaries, allowing the direct observation and evaluation of the morphology and kinetics of the solidification and the sublimation process in the same sample.

Other experimental setups for the light microscopic observation of the freezing and sublimation process (e.g. refs. [7, 32, 33]), for instance, are used to find a favourable temperature for the drying step of a freeze-drying run with a given product. As it is not possible to control the solidification front velocity and temperature gradient at the interface independently in these setups, they are not suitable for the type of experiments intended in this work.

Description of the experimental setup and performance of the experiments

The experimental setup consists of two parts. The first part is a so-called gradient freezing stage, using the Bridgman type of solidification for the freezing of the sample under steady-state conditions. The second part is a drying chamber for the sublimation dehydration of the solidified sample under isothermal conditions.

Gradient freezing stage

An experimental setup for the directional solidification of aqueous solutions and cell suspensions was designed, with the possibility of the light-microscopic observation of this process [34, 35]. The principle of such a temperature gradient microscope stage was first presented by Hunt *et al.* [36] and was introduced to low temperature biology by Rubinsky and Ikeda [37]. A sketch of this freezing stage is shown in Fig. 2. It consists of two copper blocks which are mounted at a fixed distance and kept at controlled temperatures, forming two heat reservoirs. One copper block is at a temperature above the solidification temperature of the sample under consideration, the other one at a temperature below this value. The sample, i.e. an aqueous solution, is filled into a thin and flat glass capillary (100 μm interior height, 300 μm total thickness, 1200 μm width, 10 cm length). This capillary is being pushed with constant velocity from the warm into the cold heat reservoir. In the sample a temperature profile develops, the temperature rising continuously from the value of the cold reservoir to that of the warm one. The ice–liquid interface forms at a position somewhere in the middle of the gap (10 mm) between the two heat reservoirs. Shortly after an initial transient a stationary state is reached and the ice front grows with the same velocity, v^*, the capillary is being pushed with, but in the opposite direction.

Except for a short length at the beginning and at the end of the capillary the whole length of the sample is frozen with a uniform and regular morphology not changing with position. Keeping it at low temperature to avoid melting, the capillary is removed from the freezing stage and the two ends of the capillary, which contain inhomogeneities with respect to the morphology of the frozen sample (initial and final transient), are cut off. The glass capillaries containing the frozen samples are then stored at a temperature of -196°C until they are used for drying experiments.

The interface velocity in the experiments described here is simply given by the pushing velocity of the piston. To determine the temperature gradient at the solidification interface, a one-dimensional heat transfer model is used, taking into account: the conductive heat transfer in the glass and the sample, the convective heat transfer by the movement of the pushed capillary, the latent heat formed at the solidification interface (cf. ref. [34]). The validity of this model was confirmed by temperature measurements in the sample during freezing experiments [34]. With this model, the temperature gradients at the interface for all experimental conditions under consideration are calculated. The temperatures serving as boundary conditions for this model are measured on both ends of the gap by thin copper–constantan thermocouples (wire diameter 0.2 mm) epoxied to the outer surface of the guide capillary. Figure 3 shows calculated temperature profiles in the sample capillary during solidification. A low pushing velocity is seen to result in a nearly linear temperature distribution in the sample. With a higher pushing velocity, the influence of the latent heat of solidification and of the convective heat transfer rises. In that case, the temperature gradients on the solid and the liquid side of the interface differ significantly. As proposed by Mullins and Sekerka [38], the temperature gradient G^* used for the evaluation of the solidification interface morphology is calculated by averaging the temperature gradient on the liquid G_l and the solid side G_s of the interface weighed with the thermal conductivity of the liquid and the solid, respectively

$$G^* = \frac{\kappa_s G_s + \kappa_l G_l}{\kappa_s + \kappa_l}. \tag{5}$$

In the experiments, v^* was varied from 5.5 to 34.3 μm s^{-1} and G^* from 2.0 to 7.1 K mm^{-1}.

Drying chamber

The drying chamber is designed to freeze-dry the samples previously solidified in the above described

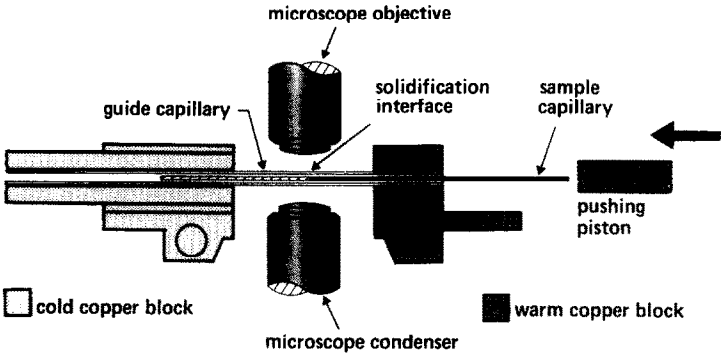

FIG. 2. Sketch of the gradient freezing stage (for further explanations see text) [34].

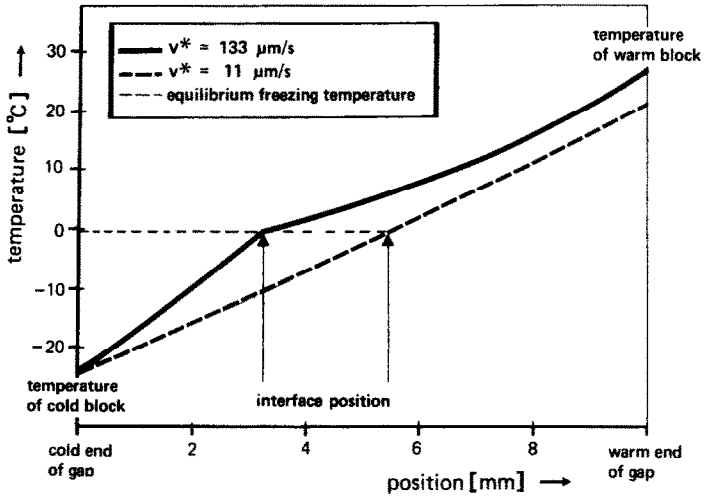

FIG. 3. Calculated temperature distribution in the sample during directional solidification at two different ice front velocities v^*.

gradient freezing stage under isothermal conditions and with the possibility of light-microscopic observation of the sublimation process. In principle the drying chamber consists of two parts (cf. Fig. 4):

(a) the sample holder;
(b) the vacuum chamber.

The sample holder ⟨1⟩ consists of a metal block, which has several drillings ⟨2⟩ through which cooled alcohol is pumped. A glass slide ⟨3⟩ is epoxied onto a longish opening in the block. The glass capillary containing the frozen sample ⟨4⟩, is attached to this slide. The block, the slide and the sample are allowed to attain the temperature of the cooling medium which is supplied and lead off through tubes ⟨10⟩. For temperature measurement in close proximity to the sample, a copper–constantan thermocouple is cemented to the slide ⟨3⟩ holding the sample.

The vacuum chamber surrounding the sample holder mainly consists of two brass parts. One part has the form of a rectangular container ⟨5⟩ and the other one forms a lid ⟨6⟩ to this container. Both,

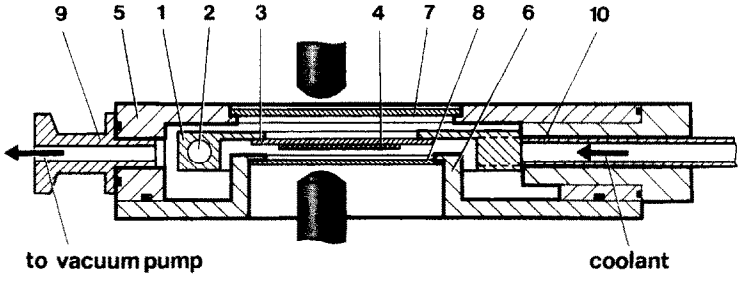

FIG. 4. Section drawing of the isothermal drying chamber (not true to scale), see text for explanations.

container and lid, bear rectangular glass windows ⟨7, 8⟩, through which the sublimation process may be observed. The container is connected to a vacuum pump by a vacuum connector ⟨9⟩.

In a cold environment, the capillaries, stored at −196°C after the solidification step, are transferred to the sample holder of the drying chamber, on which they are affixed with silicon oil to ensure a good thermal contact. The sample holder is precooled to −20°C and this value is regulated throughout the drying experiments (control measurements gave a mean temperature of -20.3 ± 0.2°C in the experiments). This temperature is chosen for the drying experiments, because on the one hand it is safely below the collapse temperature of $T_c \approx -15$°C but on the other hand it is high enough to ensure a large vapour pressure difference between sublimation interface and the surface of the sample open to the vacuum chamber. This provides for a high drying rate and at the same time simplifies the evaluation of the sublimation experiments. After locking it, the vacuum chamber is evacuated. Using a rotary vacuum pump with a displacement of 8.2 $m^3\ h^{-1}$ an absolute pressure of less than 1 Pa is always reached in the recipient after less than 5 min. The sublimation process begins at the ends of the sample, open to the vacuum chamber. The process of sublimation can be observed through a light microscope and is recorded on a videotape recorder.

From the videotape recordings taken during the freezing and drying experiments, the solidification morphology as well as the kinetics of the sublimation interface movement are evaluated.

EVALUATION OF THE EXPERIMENTS AND RESULTS

Solidification morphology

The freezing experiments are not only performed to prepare the samples for the subsequent drying experiments, but also for the evaluation of λ_1, as a function of G and v, in order to determine the proportionality constant in equation (2). For this purpose the mean distances, λ_1, of the cells or dendrites are determined from the videotape recordings taken during the freezing experiments (cf. Fig. 5 as an example of the appearance of the ice–liquid interface during the directional solidification process described above).

The directional solidification experiments are designed to investigate the primary spacing, λ_1 for values of $v^{-1/4} \cdot G^{-1/2}$ of about 0.15, 0.2, 0.25, 0.3, 0.35, 0.4, 0.45 $(\mu m\ s^{-1})^{-1/4} \cdot (K\ mm^{-1})^{-1/2}$. The real value of this freezing parameter was then evaluated from data taken during the experiments. The values of the temperatures on the warm and the cold side are measured in each experiment and with these values and the pushing velocity, the temperature gradient G^* was calculated. Not all directional solidification experiments result in a growth of the ice cells or dendrites parallel to the capillary walls. For this reason, the growth direction is taken into account in the evaluation of the experiments (cf. Fig. 6) by calculating the effective growth velocity, v_{il}, in the direction of the growth of the ice cells or dendrites from the pushing velocity, v^*, and the angle ϕ between the geometric axis of the ice cells or dendrites and the geometric axis of the sample capillary: $v_{il} = v^*/\cos\phi$ (cf. Fig. 6). In a similar way, an effective temperature gradient G is calculated from the temperature gradient G^* and the angle ϕ: $G = G^* \cdot \cos\phi$.

Figure 7 gives a compilation of the results of these measurements: the mean distance λ_1 is shown in a rectified plot vs the freezing parameters $v_{il}^{-1/4} \cdot G^{-1/2}$. For better clarity reasons, the results of each group of experiments (intended values of $v_{il}^{-1/4} \cdot G^{-1/2}$) are combined. It can be seen, that the relationship according to equation (2) is rather well fulfilled. The scatter of the λ_1 data may be partially due to the anisotropy of the ice fingers. As mentioned above, the ice fingers are supposed to have an elliptical cross-section. But only the two-dimensional projection of the ice fingers perpendicular to the growth direction may be observed and evaluated under the light microscope. Depending on the orientation of the ice fingers in the sample, the long or the short axis of the ellipse or any orientation between these extremes is observed.

Sublimation experiments

In the following, an equation is derived which was used to evaluate a diffusion coefficient for the Knudsen flow of water vapour through the dry part of the freeze-drying sample (cf. Fig. 8).

The following assumptions are made in the derivation of the equations given below:

(1) Quasi-steady-state conditions are considered here (cf. e.g. ref. [2]), i.e. it is assumed, that the movement of the receding sublimation interface has no influence on the vapour flow through the already dry part of the sample. This assumption may certainly be accepted because, as a result of the change in density, the velocity of the bulk movement of vapour escaping from the interface is six orders of magnitude larger than the velocity of the moving sublimation front at a temperature of −20°C, which was chosen for the sublimation experiments.

(2) The form of mass transfer present in the experiments as a first assumption is supposed to be Knudsen diffusion, i.e. the diffusion coefficient D for the vapour is not a function of pressure. The location, where the smallest Knudsen number exists in the experiments is in front of the interface, where the vapour pressure and thus the number of molecules per volume have a maximum. The smallest mean free path thus calculated for the sublimation temperature in our experiments (−20°C) is [39]

$$L = \frac{1}{\sqrt{2}\pi n \delta^2} = 63.7\,\mu m \qquad (6)$$

where δ is the diameter of water vapour molecules

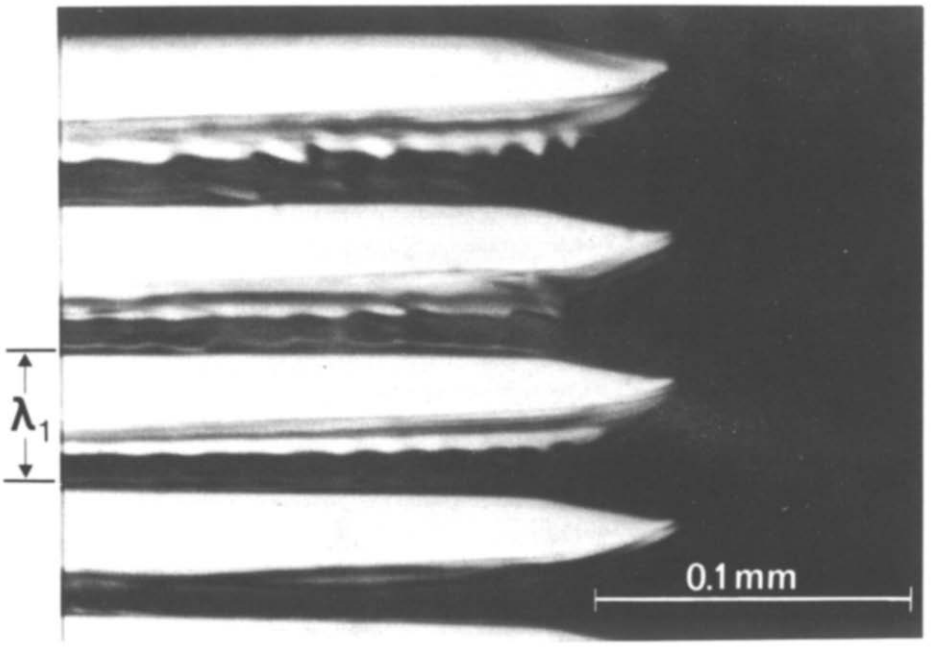

FIG. 5. Micrograph showing the morphology of the ice front during a directional solidification process in aqueous HES solution (10 wt% HES in H_2O; $v_{il} = 11\ \mu m\ s^{-1}$; $G = 3.3\ K\ mm^{-1}$) as observed with the gradient freezing stage (Bridgman type).

(here 3.46×10^{-10} m) and n the number of molecules per unit volume (here $2.953 \times 10^{22}\ m^{-3}$). With $r_e \approx \lambda_1/2$ (cf. Fig. 8) and the maximum value of the primary spacing of the ice fingers λ_1 measured in the experiments (58 μm), the minimum value of the Knudsen number is

$$Kn = \frac{L}{2r_e} = 1.09 \tag{7}$$

where r_e is the effective radius of the pores [m].

For $Kn > 1$ molecular diffusion may be assumed [40]. The value of $Kn = 1.09$ is rather near to the boundary of the Knudsen diffusion region. But this assumption may also be acceptable, because this low Knudsen number only occurs in the very proximity of the sublimation interface and only for the largest measured value of λ_1 (cf. Fig. 7).

The flux relative to the porous matrix in the one-dimensional steady-state case is given by

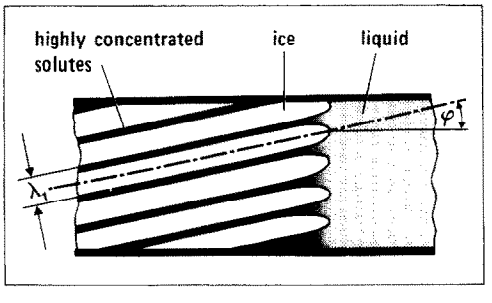

FIG. 6. Sketch explaining the evaluation of the directional solidification experiments (see text).

$$N_v = -D\frac{d\rho_v}{dx} \tag{8}$$

where N_v is the mass flux of vapour through the void part of the sample [kg $m^{-2}\ s^{-1}$], D the diffusion coefficient for vapour transport through the void part of the sample [$m^2\ s^{-1}$], ρ_v the density of water vapour [kg m^{-3}] and x the coordinate, with the origin at the sample surface and in the direction of sublimation interface movement [m] (see Fig. 8).

With the ideal gas law, the vapour density may be substituted by the vapour pressure

$$N_v = -D\frac{1}{R_v T}\frac{dp_v}{dx} \tag{9}$$

where R_v is the gas constant of vapour [J $kg^{-1}\ K^{-1}$], T the absolute temperature [K] and p_v the vapour pressure [Pa].

A mass balance at the sublimation interface expresses that the water vapour evaporated has to be transported through the dry part of the sample

$$-\rho_i\frac{dx_{iv}}{dt} = -D\frac{1}{R_v T}\left.\frac{dp_v}{dx}\right|_{(x = x_{iv})} \tag{10}$$

where ρ_i is the density of ice [kg m^{-3}], x_{iv} the position of the ice–vapour interface [m] and t the time [s].

Because of the assumed quasi-steady-state conditions the differential dp_v/dx may be substituted by a quotient of differences

$$\rho_i\frac{dx_{iv}}{dt} = D\frac{1}{R_v T}\frac{\Delta p_v}{\Delta x}. \tag{11}$$

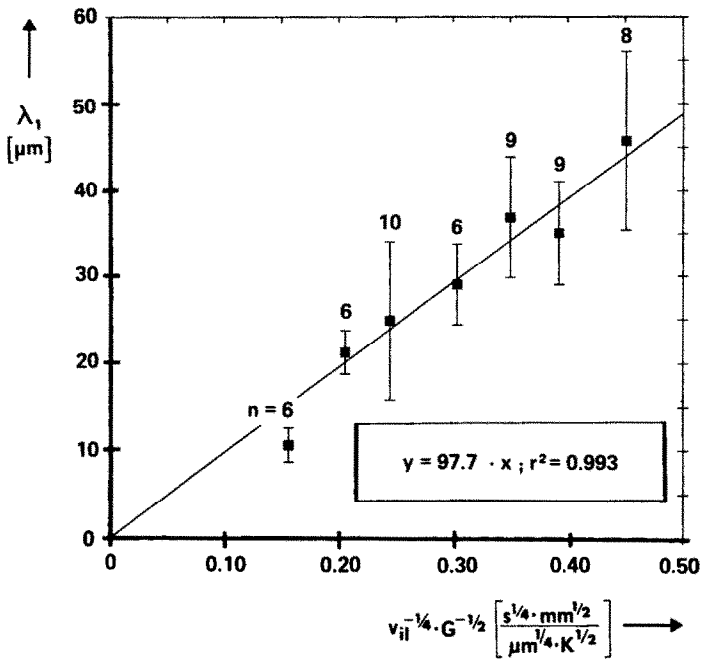

FIG. 7. Compilation of the results of the freezing experiments (10 wt% HES in H_2O): mean distances between the ice finger axes corresponding to the primary spacing λ_1. v_{il} was varied from 5.5 to 34.4 μm s^{-1}; G varied from 1.9 to 7.1 K mm^{-1}. Maximum standard deviation of x-values: 0.005 [(μm s^{-1})$^{-1/4}$ · (K mm^{-1})$^{-1/2}$].

All experiments are performed at an absolute pressure at the sample surface of 1 Pa or less. The isothermal temperature of the sample and thus the temperature of the sublimation interface was kept fixed at $-20°C$, implying that the vapour pressure at the interface was 103.2 Pa. With an error of 0.97%, the chamber pressure may be neglected in comparison to the pressure at the sublimation interface

$$\rho_i \frac{dx_{iv}}{dt} = D \frac{1}{R_v T} \frac{p_{iv}}{x_{iv}} \tag{12}$$

where p_{iv} is the vapour pressure at the interface.

Hence, after integration and with the boundary condition $x_{iv}\ (t = 0) = 0$

$$x_{iv} = \sqrt{\left(2D \frac{p_{iv} M_{H_2O}}{R_m T \rho_i}\right)} \sqrt{t} \tag{13}$$

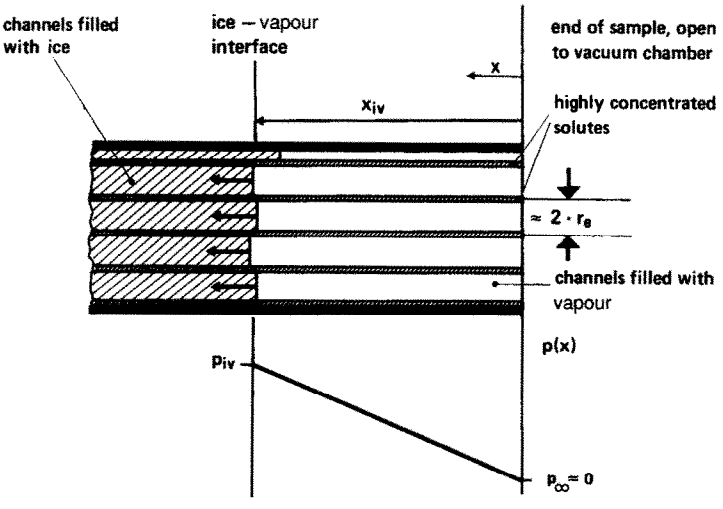

FIG. 8. Sketch explaining the evaluation of the sublimation experiments (see text).

where M_{H_2O} is the molecular weight of water [kg kmol^{-1}].

On the right-hand side of the above equation all terms are constants except time t. For this reason a rectified plot of the sublimation interface position x_{iv} vs the square root of time should result in a linear relationship. In Fig. 9 a set of photographs shows the appearance of the subliming sample in a drying experiment. Only samples are used for drying experiments in which the growth direction of the ice fingers was nearly parallel ($\phi < 5°$, cf. Fig. 6) to the capillary walls. In Fig. 10 the evaluation of three typical sublimation experiments is shown. Three lines are fitted to the experimental values, indicating that the functional relationship given in equation (13) is well satisfied. The intercept of these lines is not equal to zero. This may be explained by the experimental practice of starting the time count when opening the vacuum valve to evacuate the drying chamber. A time delay results from the fact that it takes a short time to sufficiently lower the chamber pressure to start sublimation. The first interface position vs time values are evaluated from the videotape recordings after the pressure had reached a value of less than 1 Pa in the individual experiment. From the slope of the fitted lines, the diffusion coefficients related to the freezing conditions of the specific sample could be determined.

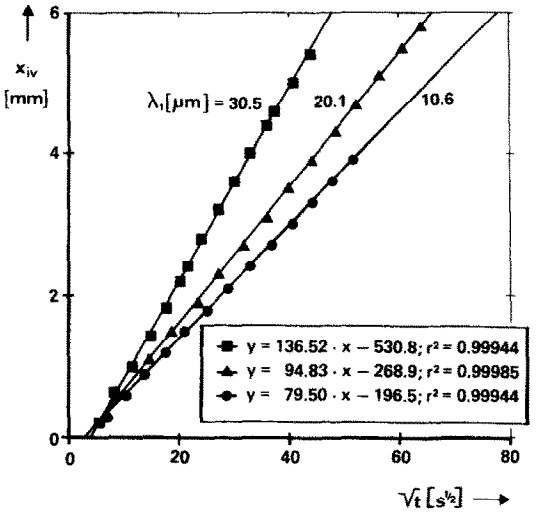

FIG. 10. Sublimation interface position, x_{iv}, vs square root of time for three experiments with different solidification patterns (v_{il} [μm s^{-1}], G [K mm^{-1}] from left to right line: 10.0, 2.1; 12.0, 6.83; 34.4, 7.1) (10 wt% HES in H_2O).

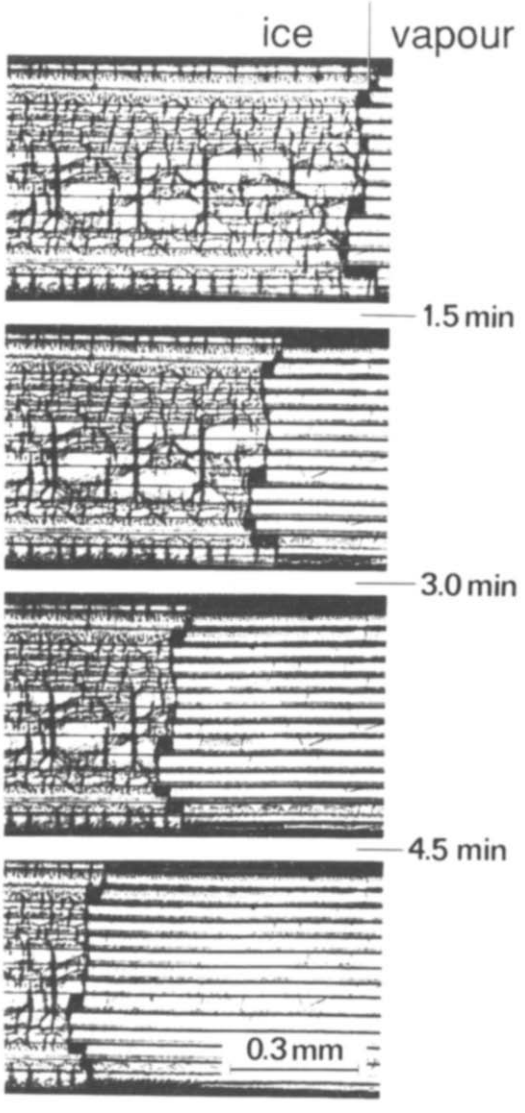

FIG. 9. Temporal sequence of micrographs taken during a sublimation experiment (10 wt% HES in H_2O, Δt = 1.5 min).

DISCUSSION AND CONCLUSIONS

In this work directional solidification experiments are performed to examine the functional relationship between the primary spacing λ_1 and the solidification parameters v_{il} and G. The proportionality between the primary spacing λ_1 and the expression $v_{il}^{-1/4} \cdot G^{-1/2}$ containing the solidification parameters (interface velocity v_{il} and temperature gradient at the interface G), as proposed by refs. [25, 41] for a regime of high interface velocities, was fitted to the experimental data. Trivedi and Somboonsuk [42] explain that the regime of high interface velocity is a regime of dendritic growth and that a decrease in interface velocity from a high value at a specific critical velocity will lead to a maximum in λ_1, and when lowered further leads to cellular growth and a steep decrease in λ_1. In this paper, no experiments are performed to examine the functional dependence of λ_1 on v_{il} at constant G. But to perform an increase in the value of $v_{il}^{-1/4} \cdot G^{-1/2}$, both v_{il} and G are varied from high to low values (cf. Fig. 7) without detecting a significant deviation from the applied functional relationship and with no distinct maximum. Thus we presume that with the values of v_{il}, chosen in our experiments, we are well in the regime of dendritic growth. A functional relationship

of the form $\lambda_1 \propto v^a \cdot G^b$ was also examined by several authors to be applicable to their experimental data. In experiments with cyclohexanol Okamoto *et al.* [43] found a relationship of $\lambda_1 \propto v^{-0.5} \cdot G^{-0.38}$ to fit best to their data. Somboonsuk *et al.* [44] found in a succinonitrile–5.5 mol% acetone system the proportionality $\lambda_1 \propto v^{-0.37 \pm 0.01}$ at a constant temperature gradient of 65 K cm^{-1} and a temperature gradient dependence of $\lambda_1 \propto G^{-0.53 \pm 0.02}$ and $\lambda_1 \propto G^{-0.43 \pm 0.02}$ for the two constant velocities 10 and 65 μm s^{-1}. Trivedi and Somboonsuk [42] compared these experimental data with the semiempirical models of Hunt [41] and Kurz and Fisher [25] (cf. equation (1)) coming to the conclusion, that there is only a poor correlation to Hunt's as well as Kurz and Fisher's theory when considering the absolute values. But in the high velocity regime they also realized only a slight deviation in slope in a λ_1 vs v diagram at constant G. Tensi and Fuchs [45] performed directional solidification experiments with two different aluminium–silicon alloys. The data obtained showed only little deviation from the functional dependence $v^{-1/4} \cdot G^{-1/2}$. Besides the results of Okamoto *et al.* [43] all the examples shown above show a relatively good agreement with the functional relationship given by the theories of Hunt [41] and Kurz and Fisher [25] in the regime of high interface velocities. It seems reasonable to fit our results of the directional solidification of an aqueous solution to the same functional relationship. The evaluation of our experimental values shows, that for the high velocity regime (dendritic growth) the theories of Hunt [41] and Kurz and Fisher [25] are also well applicable to the solidification of an aqueous solution.

From geometric considerations and from the evaluation of the experiments (cf. Fig. 9) it may be concluded, that the radius of the ice fingers, formed after complete solidification, is close to half of the dendrite spacing λ_1, but certainly proportional to this value. It was also stated (cf. equation (4)), that the diffusion coefficient in the regime of Knudsen diffusion is proportional to the radius r_e of the pore through which mass transfer is conducted. For these reasons, the prediction of a proportionality between the expression $v_{ii}^{-1/4} \cdot G^{-1/2}$ containing the solidification parameters and the diffusion coefficient D for the vapour transport during freeze-drying is proposed. Figure 11 shows the diffusion coefficients measured in the sublimation experiments plotted vs the measured primary spacing λ_1 and a line fitted to these values. Figure 12 shows the results of the sublimation experiments plotted vs the solidification parameters proposed above. A second line (fat) is added to this graph. This line represents diffusion coefficients, calculated from equation (4) and the results of the solidification experiments. The pore radius r_e (cf. equation (4)) is substituted with $\lambda_1/2$, and λ_1 is substituted with the equation describing the line fitted to the solidification experiments (cf. Fig. 7). Both lines do not differ significantly in slope. From this fact, it may be concluded, that equation (4), predicting the mass transfer through a cylindrical pore in the region of Knudsen flow, is helpful to predict mass transfer during freeze-drying in a suitable way. Surface diffusion does not seem to contribute significantly to the mass transport in our experiments.

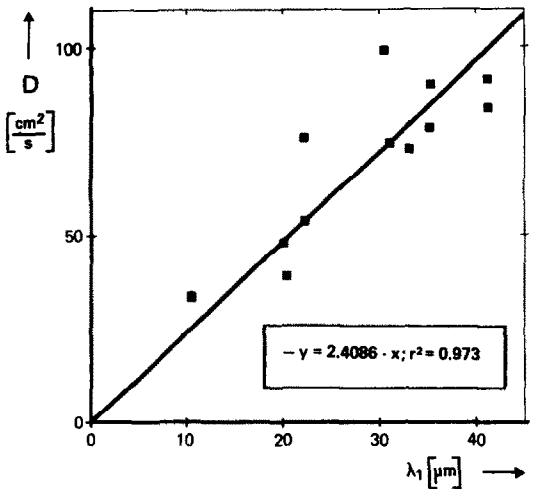

FIG. 11. Vapour diffusion coefficients, D, vs primary spacing, λ_1, determined from sublimation experiments.

A number of authors [7, 32, 46–49] observed the movement of the ice–vapour interface with the aid of a light microscope in order to study the mechanisms of vapour transport out of a freeze-drying sample qualitatively. To the knowledge of the authors of this work, there have been no publications concerning

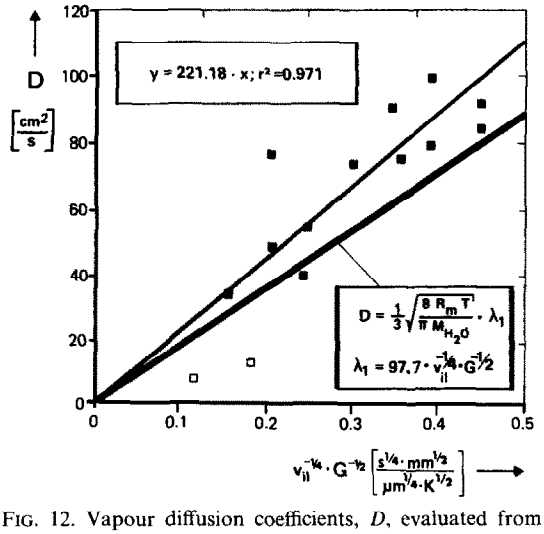

FIG. 12. Vapour diffusion coefficients, D, evaluated from sublimation experiments vs the solidification parameters $v_{ii}^{-1/4} \cdot G^{-1/2}$. Full squares: diffusion coefficients in samples without side branching. Open squares: diffusion coefficients in experiments exhibiting considerable side branching. Thin line: fitted to full squares. Fat line: diffusion coefficients predicted with the results of solidification experiments (cf. Fig. 7) and equation (4).

microscopic studies on the mass transfer during freeze-drying with quantitative results. Differences in the amount of mass transfer during freeze-drying as a result of different solidification conditions in bulk freeze-drying have been reported. Nakamura *et al.* [9] found, that the rate of freeze-drying was influenced by the freezing conditions in their experiments with coffee extract. With slower cooling rates the drying rate did not fall as significantly in the later stages of drying as they did with faster cooling. Quast and Karel [14] performed experiments on the dry layer permeability of freeze-dried coffee and of a model solution consisting of glucose, cellulose and starch. They found the permeability of the dry layer to be highest when the samples were agitated and moved during the solidification process. Their experiments on a cooling rate dependence of the dry layer permeability were difficult to interpret, because their quickly frozen samples showed extensive cracking and mass transfer during drying was performed partly through cracks. In a macroscopic sample, an increase in cooling rate normally means an increase in interface velocity and/or an increase in temperature gradient at the interface, when the other parameters (e.g. initial temperature) are kept constant. For this reason, the results obtained here seem to be consistent with those obtained by Nakamura *et al.* [9].

Relevance for bulk freeze-drying

The dependence of mass transfer during freeze-drying on the solidification parameters, v_{il} and G, was shown in this work for a wide range of these parameters. Some remarks are to be made with respect to the practical application of the results in bulk samples. For the time being, the validity of the determined proportionality constants is restricted to the model solution used in this investigation and to the mass transport being parallel to the pores of the freeze-drying sample. The solidification parameters $v_{il}^{-1/4} \cdot G^{-1/2}$ are varied in a range which we think is of practical significance. This choice of freezing parameters led to the growth of ice fingers the shape of which is characterized by trunks with nearly no side branches. The material properties of other freeze-drying additives might lead to solidification textures with the formation of side branching. With very high values of v_{il} and G our system also formed dendrites with considerable side branches. Two examples for values of the diffusion coefficient in this case are shown in the lower left of Fig. 12 (open squares). These two values demonstrate, that when side branching occurs, the diffusion coefficient D will be much lower than the experimental value determined above.

The growth direction of the ice fingers is not only determined by the heat flow direction but to a certain degree it is also controlled by the orientation of the crystallographic axes of the initial nucleus from which the ice fingers have started to grow. For this reason, not all of the fingers will grow perpendicular to a cooled bottom of a freeze-drying container, and not all of them will reach the surface of the sample in bulk freezing conditions. The growth of some of them will be stopped by the container walls or by other ice fingers crossing their growth direction. In addition, a layer of highly concentrated solutes may form on the upper surface of a sample as a result of the freezing process [2, 9, 14, 46]. For these two reasons mass transfer does not only take place through pores in a bulk freeze-drying sample, but also to a certain degree through regions of concentrated solutes.

In spite of these restrictions, we suppose that the proportionality statement obtained in this publication is a useful tool to optimize the freezing process of a freeze-drying procedure.

In our future work, we intend to investigate the applicability of the obtained results to bulk samples. This involves the numerical simulation [16, 24, 50, 51] of the freezing process in a bulk sample in order to obtain the values for v_{il} and G from simple thermal boundary conditions like a step change in temperature or a constant cooling rate B [K min^{-1}] applied to the heat exchanging bottom of the sample. We also plan to perform freeze-drying experiments in bulk samples to verify the above results for this case.

Acknowledgements—With respect to the measurements of the ice–liquid interface morphology, the partial support by the Deutsche Forschungsgemeinschaft (Grant No. Ra 335/5) is gratefully acknowledged. The authors would also like to thank the students Thomas Gremm, Jeffrey Koepele and Armin Huck for their helpful assistance.

REFERENCES

1. A. P. MacKenzie, Collapse during freeze drying—qualitative and quantitative aspects. In *Freeze Drying and Advanced Food Technology* (Edited by S. A. Goldblith, L. Rey and W. W. Rothmayr). Academic Press, New York (1975).
2. N. F. Ho and T. J. Roseman, Lyophilization of pharmaceutical injections: theoretical physical model, *J. Pharm. Sci.* **68,** 1170–1174 (1979).
3. J. Flink, The influence of freezing conditions on the properties of freeze dried coffee. In *Freeze Drying and Advanced Food Technology* (Edited by S. A. Goldblith, L. Rey and W. W. Rothmayr). Academic Press, New York (1975).
4. D. W. McPeak, E. Idziak and T. G. Smyrl, The effect of freezing rate on the retention of volatile fatty acids during freeze drying of solutions containing high molecular weight solutes, *Can. Inst. Fd Sci. Technol. J.* **20,** 176–178 (1987).
5. F. Franks, Improved freeze-drying: an analysis of the basic scientific principles, *Process Biochem.* **24,** III–VII (1989).
6. W. E. Spieß, Über den Transport des Wasserdampfes bei der Gefriertrocknung von Lebensmitteln, Doctoral Dissertation, Fak. Maschinenwesen, TH Karlsruhe (1969).
7. M. J. Pikal, S. Shah, D. Senior and J. E. Lang, Physical chemistry of freeze-drying: measurement of sublimation rates for frozen aqueous solutions by a microbalance technique, *J. Pharm. Sci.* **72,** 635–650 (1983).
8. M. J. Pikal, M. L. Roy and S. Shah, Mass and heat transfer in vial freeze-drying of pharmaceuticals: role of the vial, *J. Pharm. Sci.* **73,** 1224–1237 (1984).
9. K. Nakamura, H. Kumagai and T. Yano, Effect of freezing conditions on freeze drying rate of concentrated

liquid foods, *Fd Engng Process Appl. Transp. Phenom.* **1,** 445–450 (1986).
10. D. F. Dyer and J. E. Sunderland, Bulk and diffusional transport in the region between molecular and viscous flow, *Int. J. Heat Mass Transfer* **9,** 519–526 (1966).
11. D. F. Dyer and J. E. Sunderland, Heat and mass transfer mechanisms in sublimation dehydration, *J. Heat Transfer* **90,** 379–384 (1968).
12. S. Lin, An exact solution of the sublimation problem in a porous medium, *J. Heat Transfer* **103,** 165–168 (1981).
13. S. Lin, An exact solution of the sublimation problem in a porous medium, part II—with an unknown temperature and vapor concentration at the moving sublimation front, *J. Heat Transfer* **104,** 808–811 (1982).
14. D. G. Quast and M. Karel, Dry layer permeability and freeze-drying rates in concentrated fluid systems, *J. Fd Sci.* **33,** 70–175 (1968).
15. J. Beckmann, Ch. Körber, G. Rau, A. Hubel and E. G. Cravalho, Redefining cooling rate in terms of ice front velocity and thermal gradient: first evidence of relevance to freezing injury of lymphocytes, *Cryobiology* **27,** 279–287 (1990).
16. U. Hartmann, B. Nunner, Ch. Körber and G. Rau, Where should the cooling rate be determined in an extended freezing sample?, *Cryobiology* **28,** 115–130 (1991).
17. J. W. Rutter and B. Chalmers, A prismatic substructure forming during solidification of metals, *Can. J. Phys.* **31,** 15–39 (1953).
18. W. Kurz and D. Fisher, *Fundamentals of Solidification*, 3rd Edn. Trans Tech Publications, Aedermannsdorf, Switzerland (1989).
19. J. D. Harrison and W. A. Tiller, Controlled freezing of water. In *Ice and Snow* (Edited by W. D. Kingerey), pp. 215–225. M.I.T. Press, Cambridge, Massachusetts (1963).
20. Ch. Körber, M. W. Scheiwe and K. Wollhöver, Solute polarization during planar freezing of aqueous salt solutions, *Int. J. Heat Mass Transfer* **26,** 1241–1253 (1983).
21. K. Wollhöver, Ch. Körber, M. W. Scheiwe and U. Hartmann, Unidirectional freezing of binary aqueous solutions: an analysis of transient diffusion of heat and mass, *Int. J. Heat Mass Transfer* **28,** 761–769 (1985).
22. Ch. Körber, Phenomena at the advancing ice–liquid interface: solutes, particles and biological cells, *Q. Rev. Biophys.* **21,** 229–298 (1988).
23. Ch. Körber and M. W. Scheiwe, Observation on the non-planar freezing of aqueous salt solutions, *J. Crystal Growth* **61,** 307–316 (1983).
24. M. Jochem, U. Hartmann and Ch. Körber, Numerical solution of the coupled heat and mass transfer problem of non-planar solidification and melting in aqueous solutions, *J. Heat Transfer* (submitted).
25. W. Kurz and D. J. Fisher, Dendrite growth at the limit of stability: tip radius and spacing, *Acta Metall.* **29,** 11–20 (1981).
26. B. Nunner, Ch. Körber, G. Rau, A. Hubel and E. G. Cravalho, Characterization of phase front morphologies in aqueous solutions subjected to directional solidification, *Cryobiology* **26,** 559 (1989) (abstract, full manuscript in preparation).
27. S. H. Tirmizi and W. N. Gill, Effect of natural convection on growth velocity and morphology of dendritic ice crystals, *J. Crystal Growth* **85,** 488–502 (1987).
28. C. N. Satterfield, *Mass Transfer in Heterogeneous Catalysis*. M.I.T. Press, Cambridge, Massachusetts (1970).
29. A. Sputtek, Hydroxyethylstärke: Synthese, Eigenschaften und Anwendung als Schutzadditiv in der Kryobiologie, Doctoral Dissertation, Fak. Medizin RWTH Aachen (1990).
30. Ch. Körber, M. W. Scheiwe, P. Boutron and G. Rau, The influence of hydroxyethyl starch on ice formation in aqueous solutions, *Cryobiology* **19,** 478–492 (1982).
31. M. Jochem and Ch. Körber, Extended phase diagrams for the ternary solutions H_2O–NaCl–glycerol and H_2O–NaCl–hydroxyethylstarch (HES) determined by DSC, *Cryobiology* **24,** 513–536 (1987).
32. A. P. MacKenzie, Apparatus for microscopic observation of freeze-drying, *Biodynamica* **9,** 213–222 (1964).
33. H. Willemer, Quality control during freeze-drying of biological products, *Proc. 16th Int. Congress of Refrigeration*, Paris, France, pp. 78–83 (1983).
34. J. Beckmann, Gerichtete Erstarrung von waßrigen Lösungen und biologischen Zell-suspensionen, Diplom Thesis, Math. Naturwiss. Fakultät, RWTH Aachen (1988).
35. G. Lipp, Ch. Körber, S. Englich, U. Hartmann and G. Rau, Investigation of the behavior of dissolved gases during freezing, *Cryobiology* **24,** 489–503 (1987).
36. J. D. Hunt, K. A. Jackson and H. Brown, Temperature gradient microscope stage suitable for freezing materials with melting points between −100 and +200°C, *Rev. Scient. Instrum.* **37,** 805 (1966).
37. B. Rubinsky and M. Ikeda, A cryomicroscope using directional solidification for the controlled freezing of biological material, *Cryobiology* **22,** 55–68 (1985).
38. W. W. Mullins and R. F. Sekerka, Stability of a planar interface during solidification of a dilute binary alloy, *J. Appl. Phys.* **35,** 444–451 (1964).
39. S. Chapman and T. G. Cowling, *The Mathematical Theory of Non-uniform Gases*. The University Press, Cambridge, U.K. (1939).
40. J. D. Mellor and D. A. Lovett, Flow of gases through channels with reference to porous materials, *Vacuum* **18,** 625–627 (1968).
41. J. D. Hunt, Cellular and primary dendrite spacings, *Solidification and Casting of Metals, Proc. Int. Conf. on Solidification*, Sheffield, U.K., pp. 3–9. The Metals Society, London, U.K. (1979).
42. R. Trivedi and K. Somboonsuk, Pattern formation during the directional solidification of binary systems, *Acta Metall.* **33,** 1061–1068 (1985).
43. T. Okamoto, K. Kishitake and I. Bessho, Dendritic structure in unidirectionally solidified cyclohexanol, *J. Crystal Growth* **29,** 131–136 (1975).
44. K. Somboonsuk, J. T. Mason and R. Trivedi, Interdendritic spacing: part I. Experimental studies, *Metall. Trans.* **15a,** 967–975 (1984).
45. H. M. Tensi and H. Fuchs, Beeinflussung der mechanischen Eigenschaften von Aluminium–Silicium-Gußlegierungen durch Erstarrrungsparameter und Gefügestruktur, *Gießereiforschung* **35,** 61–68 (1983).
46. M. Kochs, P. Schwindke and Ch. Körber, A microscope stage for the dynamic observation of freezing and freeze-drying in solutes and cell suspensions, *Cryo-Letters* **12,** 401–419 (1989).
47. F. Chauffard, Microscopical examination of freezing and freeze-drying, *Nestlé Res. News* **1971,** 78–80 (1971).
48. J. Flink and F. Gejl-Hansen, Two simple freeze drying microscope stages, *Rev. Scient. Instrum.* **49**(2), 269–271 (1978).
49. A. P. MacKenzie, Factors affecting the transformation of ice into water vapor in the freeze-drying process, *Ann. N.Y. Acad. Sci.* **123,** 522–547 (1965).
50. U. Hartmann, Wärmetechnische Aspekte des Gefrierens bei der Kryokonservierung lebender Zellen, Doctoral Dissertation, Fak. Maschinenwesen, RWTH Aachen (1987).
51. M. Jochem, U. Hartmann and Ch. Körber, Modeling of coupled heat and mass transfer problem of nonplanar solidification and melting in aqueous solutions and numerical treatment. In *Network Thermodynamics, Heat and Mass Transfer in Biotechnology* (Edited by K. R. Diller), pp. 73–80. American Society of Mechanical Engineers, New York (1987).

INFLUENCE DU MECANISME DE GEL SUR LE TRANSPORT DE VAPEUR PENDANT LA SUBLIMATION EN LYOPHILISATION

Résumé—On étudie l'influence du mécanisme de gel sur le transfert de masse pendant la sublimation dans une solution aqueuse de polymère. On considère différentes textures d'échantillon gelé dépendant des paramètres de solidification et du coefficient de diffusion qui dépend de la structure, pour le transport de vapeur hors de l'échantillon gelé en assèchement. Des expériences sont conduites en utilisant une méthode de solidification directionnelle contrôlée (technique de Bridgman) et une sublimation isotherme analysée à l'aide d'un microscope. On montre la dépendance de l'espacement primaire λ_1 du doigt de glace, vis-à-vis du paramètre $v_{il}^{-1/4} \cdot G^{-1/2}$ (Hunt, *Solidification and Casting of Metals, Proc. Int. Conf. on Solidification*, Sheffield, U.K., pp. 3–9. The Metals Society (1979); Kurz and Fisher, *Acta Metall.* **29**, 11–20 (1981)). Une proportionalité entre cette combinaison des paramètres du gel et le coefficient de diffusion pour le transport de vapeur pendant la sublimation est confirmée par l'expérience.

DER EINFLUSS DES GEFRIERVORGANGS AUF DEN DAMPFTRANSPORT BEI DER SUBLIMATION WÄHREND DER GEFRIERTROCKNUNG IM VAKUUM

Zusammenfassung—Es wird der Einfluß des Gefriervorgangs auf den Stofftransport bei der nachfolgenden Sublimation in einer wäßrigen Polymerlösung untersucht. Die unterschiedlichen Gefügeformen in der gefrorenen Probe werden studiert, die sich abhängig von den Verfestigungsparametern und vom gefügeabhängigen Diffusionskoeffizienten für den Dampftransport aus der gefrorenen, trocknenden Probe heraus ergeben. Bei den Versuchen wird ein geregeltes, gerichtetes Verfestigungsverfahren (Bridgman-Technik) und isotherme Sublimation verwendet. Die Untersuchung erfolgt mit Hilfe eines Lichtmikroskops. Die Abhängigkeit des anfänglichen Abstands λ_1 der 'Eisfinger' von den Verfestigungsparametern wird gezeigt ($v_{il}^{-1/4}G^{-1/2}$; Geschwindigkeit und Temperaturgradient an der Verfestigungsfront). (Hunt, *Solidification and Casting of Metals, Proc. Int. Conf. on Solidification*, Sheffield, U.K., pp. 3–9. The Metals Society (1979); Kurz and Fisher, *Acta Metall.* **29**, 11–20 (1981).) Die Versuche bestätigen die Proportionalität zwischen der angegebenen Kombination der Verfestigungsparameter und dem Diffusionskoeffizienten für den Dampftransport während der Sublimation.

ВЛИЯНИЕ ПРОЦЕССА ЗАМОРАЖИВАНИЯ НА ПЕРЕНОС ПАРА В УСЛОВИЯХ ВАКУУМНО-СУБЛИМАЦИОННОЙ СУШКИ

Аннотация—Исследуется влияние процесса замораживания на массоперенос при последующей сублимации в водном растворе полимера. Рассматривается перенос пара из образца для различных текстур, обусловленных параметрами процесса замораживания, при зависящем от текстуры коэффициенте диффузии. В экспериментах используются метод регулируемого направленного затвердевания (метод Бридгмэна) и изотермическая сублимация, наблюдаемая с помощью оптического микроскопа. Показана зависимость первоначального интервала λ_1 между "ледяными пальцами" от параметров затвердевания $v_{il}^{-1/4} \cdot G^{-1/2}$ (Hunt, *Solidification and Casting of Metals, Proc. Int. Conf. on Solidification*, Sheffield, U.K., pp. 3–9. The Metals Society (1979); Kurz and Fisher, *Acta Metall.* **29**, 11–20 (1981)). Экспериментально подтверждена пропорциональность между данной комбинацией параметров замораживания и коэффициентом диффузии для переноса пара при сублимации.